resented in Table II was also followed with MP3.[14] As seen in Figure 2, this additional correction lowers the barrier to 8.5 kcal/mol. To investigate the effect of using 3-21G geometries, the structures at $\alpha = 180°$, 120°, and 90° were recalculated with the use of the 6-31G* basis set. As expected,[13] the main effect is to shorten the C–Si bond at all angles. The energy results are summarized in Table III. As before the SCF curve finds no barrier, while a barrier does appear at both MP2 and MP3 levels. The energy difference between $\alpha = 120°$ and $\alpha = 90°$ is only slightly reduced at both MP2 and MP3 (relative to Figure 2). Further, the addition of p functions on the hydrogens (6-31G**//6-31G*) has a very small effect at both the SCF and MP2 levels. Thus, it appears that there may be a significant barrier separating silaethyne and silylidene.

Since the perturbation correction corresponds to the addition of a large number of doubly excited configurations to the SCF wave function,[8] it is difficult to find a straightforward interpretation of the effect. A *qualitative* understanding may be obtained by simply carrying out a 2 × 2 CI, including the SCF configuration and the double excitation which removes a pair of electrons from the highest occupied orbital (HOMO) and places them in the lowest unoccupied orbital (LUMO). The latter orbital is one of two degenerate π^* MO's at $\alpha = 180$ and becomes a p_x antibonding orbital with a small mixing of s character as α decreases (the HOMO is the bonding counterpart). The effect of adding the second configuration at $\alpha = 140°$ and $\alpha = 88.6°$ is to change the energy difference ($E(\alpha = 88.6°) - E(\alpha = 140°)$) from −5.9 kcal/mol at the SCF(6-31G*) level to +6.1 kcal/mol. A further analysis reveals that the orbital energy of the LUMO is rather small (<0.1) throughout the surface and that the HOMO–LUMO splitting increases from $\alpha = 140°$ to $\alpha = 60°$. The small HOMO–LUMO splitting at all angles (about half that of acetylene) will give rise to unusually large interaction between the two configurations. Since the SCF surface is rather flat in the region from $\alpha = 140°$ to $\alpha = 80°$, this region may well be dominated by variations in the HOMO–LUMO interaction. A more quantitative analysis would require a study of all contributing configurations.

To summarize, the major findings of this work are as follows: (a) the carbon–silicon triple bond is particularly unstable in a thermodynamic sense, as is evidenced by the calculated hydrogenation energies and by the isomerization energy relative to silylidene. (b) At the highest level of computation, a slightly bent form of silaethyne is found to be separated from its more stable isomer by a small barrier. It should be recognized, however, that the height of the barrier might be altered by higher order effects or by a modification of the reaction path due to correlation effects.

Acknowledgment. This work was supported by National Science Foundation Grants No. CHE78-18070 and CHE77-09293 and by a generous allotment of computer time from the North Dakota State University Computer Center. One of us (M.S.G.) has benefitted from interactions with Professors R. D. Koob and P. Boudjouk during the course of this work.

Sensitivity of Polypeptide Conformation to Geometry. Theoretical Conformational Analysis of Oligomers of α-Aminoisobutyric Acid

Yvonne Paterson,[1a] Shirley M. Rumsey,[1a] Ettore Benedetti,[1b] George Némethy,[1a] and Harold A. Scheraga*[1a]

Contribution from the Baker Laboratory of Chemistry, Cornell University, Ithaca, New York 14853, and Istituto Chimico, Università di Napoli, 80134 Napoli, Italy.
Received October 10, 1980

Abstract: Empirical observations by other workers have suggested that peptides containing α-aminoisobutyric acid obligatorily adopt 3_{10}-helical forms in the crystal state. The reasons for this conformational preference have not been understood heretofore, and this question is addressed in the present study. The preferred conformations of *N*-acetyl-*N'*-methyl(α-aminoisobutyryl)$_n$amide (with $n = 1, 2, 3$) have been determined by empirical conformational energy calculations; minimum energy conformations were located by minimizing the energy with respect to all the dihedral angles of the molecule. The conformational space of the α-aminoisobutyric acid residue is sterically severely restricted and therefore sensitive to the covalent geometry assigned to this residue, in particular to the bond angles between the substituents on the C^α atom. Tetrahedral symmetrical geometry for these substituents favors the α-helical conformation for the α-aminoisobutyric acid residue (and di- and tripeptides thereof) whereas asymmetric geometry, derived from well-refined X-ray structures, gives the 3_{10} conformation as the preferred structure. Analysis of pairwise atomic interactions indicates that favorable backbone–backbone interactions lower the overall energy of the molecule in the 3_{10} conformation when the substitution on the C^α atom is asymmetric.

The wide occurrence of α-aminoisobutyric acid (abbreviated Aib) in microbial peptides, particularly in the peptaibophols,[2,3] has long been attributed to its role in constraining the peptide backbone, because of the two methyl substituents on the C^α atom. Recent experimental work has demonstrated unequivocally that the Aib residue in peptide crystals always occurs in the right- or left-handed 3_{10}-helical conformation;[4-12] this is in conflict with early theoretical studies[13-15] of the Aib residue, using confor-

(1) (a) Baker Laboratory of Chemistry, Cornell University. (b) Istituto Chimico, Università di Napoli.
(2) Pandey, R. C.; Meng, H.; Cook, J. C.; Rinehart, K. L. *J. Am. Chem. Soc.* **1977**, *99*, 5203–5205.
(3) Pandey, R. C.; Cook, J. C.; Rinehart, K. L. *J. Am. Chem. Soc.* **1977**, *99*, 5205–5206.
(4) Flippen, J. L.; Karle, I. L. *Biopolymers* **1976**, *15*, 1081–1092.
(5) Shamala, N.; Nagaraj, R.; Balaram, P. *Biochem. Biophys. Res. Comm.* **1977**, *79*, 292–298.
(6) Shamala, N.; Nagaraj, R.; Balaram, P. *J. Chem. Soc., Chem. Commun.* **1978**, 996–997.
(7) Aubry, A.; Protas, J.; Boussard, G.; Marraud, M.; Néel, J. *Biopolymers* **1978**, *17*, 1693–1711.
(8) Prasad, B. V. V.; Shamala, N.; Nagaraj, R.; Chandrasekaran, R.; Balaram, P. *Biopolymers* **1979**, *18*, 1635–1646.
(9) Nagaraj, R.; Shamala, N.; Balaram, P. *J. Am. Chem. Soc.* **1979**, *101*, 16–20.

0002-7863/81/1503-2947$01.25/0

mational energy calculations, which suggest that this residue is obliged to adopt either the right- or the left-handed α-helical conformation. A more recent calculation[16] of a polymeric form of Aib showed that the two α-helical conformations were energetically more favorable than the two 3_{10}-helical conformations for poly(Aib). All of these studies, however, used potential functions with older parameters which were based on limited data. The present study was therefore carried out in order to analyze the geometrical and energetic factors that govern the conformations of the Aib residue and thus to determine why the 3_{10} is more stable than the α-helical conformation.

The values of the backbone dihedral angles ϕ and ψ, required to generate an ideal α helix, $(\phi,\psi) = (-55°,-45°)$, and an ideal 3_{10} helix, $(\phi,\psi) = (-60°,-30°)$, are very close to each other. The two helices differ essentially in their pattern of hydrogen bonding. In the α helix, there is a hydrogen bond between the amide hydrogen of a given residue and the carbonyl oxygen of the fourth preceding residue ($i \rightarrow i-4$ hydrogen bond), while the hydrogen bond in the 3_{10} helix involves the carbonyl oxygen of the third preceding residue ($i \rightarrow i-3$ hydrogen bond).[17] Relatively small variations of ϕ and ψ will change the hydrogen-bonding pattern.

Since the Aib residue is so sterically hindered, the extent of freedom of its backbone dihedral angles will be very sensitive to the covalent geometry used for this residue and the potential functions used to calculate the contribution of the nonbonded interaction energies to the total energy. In addition, the prediction of preferences of one hydrogen-bonded conformation over another will be strongly influenced by the choice of potential function to represent hydrogen-bond interactions between relevant groups.

In this study, we use conformational energy calculations to establish that the preferred conformation of the *N*-acetyl-*N'*-methyl amides of Aib_2 and Aib_3 is a 3_{10} helix. We use conformational energy parameters[18] (employed in the computer program ECEPP[19]) to describe the conformational space available to both the backbone and side chain of these peptides. These parameters have been refined more recently than those used in the studies cited above. The influence of changes in covalent geometry on this conformational space and the energetics and geometry of the hydrogen bond in these peptides is demonstrated and discussed.

Methods

Nomenclature. The C^β carbon atom of Aib that occupies the same position as the C^β carbon atoms in L-amino acids is designated as C^β_L. The C^β carbon atom that substitutes for the α hydrogen atom in L-amino acids is designated as C^β_D. All other nomenclature is that recommended by the IUPAC–IUB Commission.[17]

Residue Geometry (Bond Lengths and Bond Angles). The standard end group geometry of ECEPP[19] was used for the *N*-acetyl and *N'*-methyl end groups. Two geometries were used for the Aib residue; one is referred to as symmetric and the other as asymmetric. They differ only in the bond angles between the substituent atoms on the C^α atom. All other bond angles and all bond lengths are taken from standard ECEPP geometry for amino acid residues. For the symmetric geometry, the four heavy-atom substituents on the C^α atom are positioned tetrahedrally, i.e., $\tau(NC^\alpha C^\beta_D) = \tau(NC^\alpha C^\beta_L) = \tau(NC^\alpha C') = \tau(C^\beta_L C^\alpha C^\beta_D) = \tau(C^\beta_D C^\alpha C') = \tau(C^\beta_L C^\alpha C') = 109.45°$.

An asymmetric geometry was also tested, because it corresponds more closely to that of the Aib residue in crystal structures of peptides containing this residue. In order to obtain the bond lengths and bond angles for this asymmetric arrangement, the crystal data of well refined ($R \leq 0.08$) structures of peptides containing the Aib residue were reviewed, and 17 observations were averaged (Tables I and II). The average values of all bond lengths (Table I) and bond angles (Table II) of the peptide group are consistent with the values used by ECEPP. In crystal structures where the Aib residue adopts a right-handed helical conformation (i.e., ϕ and ψ have negative values), however, $\tau(NC^\alpha C^\beta_L)$ and $\tau(C^\beta_L C^\alpha C')$ are significantly less than the tetrahedral values, and $\tau(NC^\alpha C^\beta_D)$ and $\tau(C^\beta_D C^\alpha C')$ are significantly greater than the tetrahedral values. In crystal structures where the Aib residue adopts a left-handed helical structure, the reverse is true. In other words, there is an intimate connection between the conformation and the geometry of the Aib residue. In order to demonstrate the consistent nature of this departure from the tetrahedral values, and in order to obtain average values of the bond angles for use in the computations, all bond angles with positive and negative deviations from the tetrahedral values have been grouped together in Table II; i.e., the values of the bond angles involving C^β_D and C^β_L atoms have been interchanged for residues in the left-handed conformations. The average values for the bond angles between the substituents on the C^α atom, listed in Table II, were used for the asymmetric geometry of the Aib residue. All other bond lengths and bond angles are taken from ECEPP.

Potentials and Energy Parameters. Conformational energies were calculated by using ECEPP[19] which employs the empirical potential-energy functions and energy parameters derived by Momany et al.[18] Partial charges of the Aib residue were obtained from CNDO/2 calculations, performed[18] on the *N*-acetyl-*N'*-methyl amide of Aib, using both the symmetric and asymmetric geometry in the fully extended and α-helical conformations. Partial charges for the residue from these calculations were not significantly different for either of the conformations or the geometries considered. The partial charges for the backbone atoms, except for the C^α atom, were close to those derived for other amino acid residues,[18] and the ECEPP values for these were used. The following values were used for the C^α atom and its substituents: C^α 0.113, C^β –0.132, H^β 0.044 ecu, where ecu is electronic charge unit. They render the residue electrically neutral.

The total conformational energy E calculated by ECEPP is the sum of the electrostatic energy E_{ES}, the nonbonded energy E_{NB}, and the torsional energy E_{TOR}.[18] The hydrogen-bond energy is included in the nonbonded energy component.[18,19] Hydrogen atoms are considered explicitly in all interactions. Strain energy, corresponding to changes in bond angles, was not calculated in this work. Conformational energies are expressed as $\Delta E = E - E_0$, where E_0 is the energy of the lowest energy conformation for a given geometry.

Location of Low-Energy Conformations. The conformational space of the terminally blocked single residue Ac-Aib-NHMe was mapped by calculating the conformational energy at 10° intervals of ϕ and ψ, i.e., at 1296 points in the ϕ,ψ plane. The side-chain methyl torsional angles were held fixed in the "staggered" position of the torsional minima, i.e., $\chi^{1,1} = \chi^{1,2} = 180°$. The dihedral angles about the peptide bonds (ω) and of the two end methyl groups were held fixed[20] at 180°.

The exploration of the conformational space of the terminally blocked dipeptide Ac-Aib_2-NHMe was shortened, in order to save computational time, by using several restrictive conditions which reduce the number of independent variables, as follows: (a) $\phi_1 = \phi_2$ and $\psi_1 = \psi_2$, i.e., regularly repeating conformations. (b) $\phi_1 = -\phi_2$ and $\psi_1 = -\psi_2$, i.e., the conformation of the second residue

(10) Prasad, B. V. V.; Shamala, N.; Nagaraj, R.; Balaram, P. *Acta Crystallogr., Sect. B* **1980**, *B36*, 107–110.
(11) Smith, G. D.; Pletnev, V. Z.; Duax, W. L.; Balasubramanian, T. M.; Bosshard, H. E.; Czerwinski, E. W.; Kendrick, N. E.; Matthews, F. S.; Marshall, G. R. *J. Am. Chem. Soc.* **1981**, *103*, 1493.
(12) Benedetti, E.; Pedone, C.; Toniolo, C. *Pept. Proc. Eur. Pept. Symp., 16th, 1980*, in press.
(13) Marshall, G. R.; Bosshard, H. E. *Circ. Res., Suppl. II* **1972**, *30* and *31*, 143–150.
(14) Pletnev, V. Z.; Gramov, E. P.; Popov, E. M. *Khim. Prir. Soedin.* **1973**, 224–229.
(15) Burgess, A. W.; Leach, S. J. *Biopolymers* **1973**, *12*, 2599–2605.
(16) Prasad, B. V. V.; Sasisekharan, V. *Macromolecules* **1979**, *12*, 1107–1110.
(17) IUPAC–IUB Commission on Biochemical Nomenclature, *Biochemistry* **1970**, *9*, 3471–3479.
(18) Momany, F. A.; McGuire, R. F.; Burgess, A. W.; Scheraga, H. A. *J. Phys. Chem.* **1975**, *79*, 2361–2381.
(19) The Fortran computer program for ECEPP, its description, and all associated geometric and energy parameters are available on magnetic tape (No. QCPE 286) from the Quantum Chemistry Program Exchange, Indiana University, Bloomington, IN.
(20) Zimmerman, S. S.; Pottle, M. S.; Němethy, G.; Scheraga, H. A. *Macromolecules* **1977**, *10*, 1–9.

Table I. Bond Lengths (Å) for the Aib Residue in Published Crystal Structures of Peptides

	ref	C'–N	N–C^{α}	C^{α}–C'	C'=O	C^{α}–$C^{\beta}{}_{D}$	C^{α}–$C^{\beta}{}_{L}$
Boc-Aib-OH	12	1.336	1.465	1.538	1.326	1.530	1.528
Z-Aib_2-OH	12	1.352	1.463	1.531	1.239	1.535	1.544
		1.342	1.467	1.530	1.306	1.533	1.544
Z-Aib_4-OH	12	1.359	1.465	1.533	1.222	1.533	1.526
		1.350	1.468	1.550	1.213	1.529	1.538
		1.351	1.478	1.538	1.227	1.520	1.538
		1.339	1.462	1.542	1.195	1.523	1.533
Z-Aib_5-OBu^t	12	1.339	1.464	1.535	1.221	1.533	1.527
		1.347	1.464	1.533	1.232	1.531	1.536
		1.338	1.467	1.541	1.228	1.520	1.532
		1.344	1.471	1.542	1.229	1.525	1.531
		1.333	1.462	1.516	1.198	1.528	1.538
Z-Aib-Pro-NHMe	8	1.335	1.470	1.536	1.234	1.510	1.538
Z-Aib_2-Ala-OH	10	1.339	1.465	1.540	1.233	1.536	1.543
		1.333	1.481	1.543	1.240	1.535	1.528
Boc-Gly-Aib-OH	11	1.332	1.466	1.538	1.209	1.524	1.535
Boc-Leu-Aib-Pro-OH	11	1.312	1.533	1.513	1.232	1.492	1.535
average		1.340	1.47	1.54	1.23	1.53	1.53
standard deviation		±0.010	±0.016	±0.009	±0.030	±0.010	±0.006
ECEPP values	18	1.325	1.45	1.53	1.23		1.53

Table II. Bond Angles (deg) for the Aib Residue in Published Crystal Structures of Peptides Normalized to Right-Handed Helical Structures

		chirality of	bond angles around α-carbon atom						bond angles around peptide group atoms			
	ref	residue[a]	$\tau(N_iC^{\alpha}{}_iC')$	$\tau(N_iC^{\alpha}{}_iC^{\beta}{}_L)$[b]	$\tau(N_iC^{\alpha}{}_iC^{\beta}{}_D)$[b]	$\tau(C^{\beta}{}_LC^{\alpha}{}_iC^{\beta}{}_D)$	$\tau(C^{\beta}{}_LC^{\alpha}{}_iC'_i)$[c]	$\tau(C^{\beta}{}_DC^{\alpha}{}_iC'_i)$[c]	$\tau(C^{\alpha}{}_iC'_iO_i)$	$\tau(C^{\alpha}{}_iC'_iN_{i+1}$	$\tau(O_iC'_iN_{i+1})$	$\tau(C'_{i-1}N_iC^{\alpha}{}_i)$
Boc-Aib-OH	12	R	110.5	106.8	110.4	111.3	107.4	110.3		no $i+1$ residue		122.3
Z-Aib_2-OH	12	L	112.3	106.2	112.4	110.6	106.3	108.8	120.4	117.7	121.6	123.9
		R	108.9	107.7	111.1	111.3	106.1	112.2		no $i+1$ residue		120.8
Z-Aib_4-OH	12	R	112.5	107.3	110.2	110.7	107.1	108.9	120.5	117.8	121.6	120.8
		R	111.9	106.4	111.3	110.7	107.6	108.9	120.2	116.5	123.2	122.2
		R	111.1	107.3	110.8	109.6	106.2	111.6	121.0	116.3	122.5	122.0
		L	111.9	107.8	109.9	111.4	106.2	109.6		no $i+1$ residue		124.2
Z-Aib_5-OBu^t	12	R	111.7	107.3	110.9	110.4	107.3	109.2	121.3	116.4	122.3	121.4
		R	110.2	107.3	110.7	110.6	107.4	110.4	120.4	116.5	123.0	122.9
		R	111.3	107.3	110.8	109.9	106.3	111.0	120.8	116.1	123.0	122.1
		R	111.1	107.2	112.0	110.3	105.7	110.3	120.5	116.7	122.6	123.1
		L	111.5	107.0	111.1	110.2	106.5	110.4		no $i+1$ residue		122.2
Z-Aib-Pro-NHMe	8	R	111.0	107.6	110.1	111.1	106.6	110.4		$i+1$ residue is proline		122.9
Z-Aib_2-Ala-OH	10	L	111.5	107.1	110.2	110.6	106.2	111.1	119.4	117.5	123.0	121.2
		L	111.0	107.4	111.4	108.6	107.6	110.6	119.7	116.7	123.0	123.5
Boc-Gly-Aib-OH	11	L	109.1	107.5	111.3	111.5	106.8	110.5		no $i+1$ residue		121.6
Boc-Leu-Aib-Pro-OH	11	L	111.6	104.6	107.0	111.5	107.3	114.4		$i+1$ residue is proline		119.0
av			111.1	107.0	110.7	110.6	106.7	110.5	120.4	116.8	122.6	122.1
standard deviation			±0.96	±0.73	±1.12	±0.74	±0.59	±1.34	±0.5	±0.6	±0.6	±1.20
ECEPP values	18		111.0 (Gly) 109.3 (Ala)						120.5	115.0	124.5	121.0

[a] R = right chirality; the values of both ϕ and ψ are negative in the crystal. L = left chirality; the values of both ϕ and ψ are positive in the crystal. [b,c] The values of these two bond angles have been interchanged in these columns for all residues with L chirality, for reasons explained in the text.

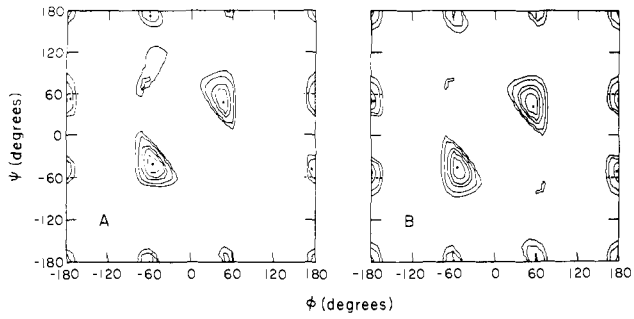

Figure 1. Conformational energy contour maps of Ac-Aib-NHMe for (A) asymmetric and (B) symmetric geometry, with fixed $\omega_0 = \omega_1 = \chi^{1,1} = \chi^{1,2} = 180°$. The contour lines are drawn at 1, 3, 5, 10, and 15 kcal/mol above the 10° grid point of lowest energy for each map, located at $(\phi,\psi) = (-50°,-40°)$ in part A and $(\pm 50°,\pm 50°)$ in part B. Locations of minimum-energy conformations, obtained with variable ω's and χ's (listed in Table III), are indicated by the filled circles. See the text for discussion of equivalent enantiomeric conformations in the case of asymmetric geometry.

is the mirror image of that of the first residue. (c) ϕ_1 and ψ_2 were assigned fixed values, chosen from the low-energy minima of the terminally blocked single residue (Table III), and only ψ_1 and ϕ_2, the dihedral angles next to the central peptide unit, were treated as variables. The conformational energy was calculated at 10° intervals of the variable dihedral angles in each case. Condition a produced the lowest energy minima and the widest low-energy conformational space for the backbone of the dipeptide. Consequently, this was the only condition used in the exploration of the conformational space of the terminally blocked tripeptide Ac-Aib$_3$-NHMe.

Low-energy regions were located on energy contour maps for conditions a, b, and c for Ac-Aib$_2$-NHMe and condition a for Ac-Aib$_3$-NHMe. Minimum energy conformations were then obtained in all of these regions by minimizing the energy with respect to all dihedral angles of each residue, i.e., ϕ, ψ, ω, $\chi^{1,1}$ and $\chi^{1,2}$, using ECEPP in conjunction with a function-minimizing subroutine MINOP.[21] The dihedral angles of the end groups, however, were held fixed[20] at 180°. Minimization was terminated when the conformational energy changed by less than 0.001 kcal/mol between successive calculations.

Hydrogen Bonds. Each minimum-energy conformation was analyzed for possible backbone–backbone hydrogen bonds by calculating all H···A distances where H is a polar hydrogen atom and A is a proton acceptor (an oxygen or nitrogen atom). If the H···A distance is less than or equal to 2.3 Å, the two atoms are considered to be involved in a hydrogen bond.[20]

The influence of the value of $\tau(NC^{\alpha}C')$ on the propensity of the peptide backbone to form hydrogen bonds in the 3_{10}- and α-helical conformations was explored. The (N)H···O distances of the $i \rightarrow i-3$ and $i \rightarrow i-4$ hydrogen bonds for the regularly repeating conformations of Ac-Aib$_3$-NHMe were calculated, using both the asymmetric and the symmetric backbone geometry. These (N)H···O distances computed at 2° increments of ϕ and ψ were plotted for an area of the ϕ,ψ map that encompasses both the 3_{10}- and α-helical conformations, i.e., the square enclosed between 0 and −90° in both ϕ and ψ; ω was kept constant at 180°. Contours of constant hydrogen bond length were plotted from 1.7 to 2.3 Å. This range includes all normal hydrogen-bonding distances, because the distance at which the minimum in the hydrogen bond potential occurs for the amide hydrogen and carbonyl oxygen[22] is 1.90 Å and the distance at which the potential energy is zero is 1.73 Å.

Results

Conformational Space and Minimum-Energy Conformations of Ac-Aib$_n$-NHMe with n = 1, 2, and 3. Figure 1A,B gives the

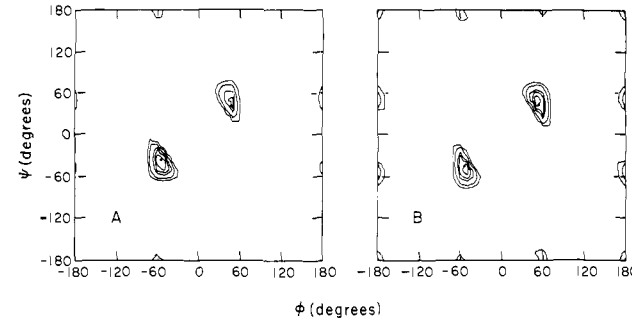

Figure 2. Conformational energy contour maps of regularly repeating conformations ($\phi_1 = \phi_2$ and $\psi_1 = \psi_2$) of Ac-Aib$_2$-NHMe for (A) asymmetric and (B) symmetric geometry, with all values of ω and χ fixed at 180°. The contour lines are drawn at 1, 3, 5, 10, and 15 kcal/mol above the 10° grid point of lowest energy for each map, located at $(\phi,\psi) = (-60°,-30°)$ in part A and $(-50°,-50°)$ in part B. Locations of minimum-energy conformations, obtained with variables ω's and χ's (listed in Table IV), are indicated by the filled circles. See the text for discussion of equivalent enantiomeric conformations in the case of asymmetric geometry.

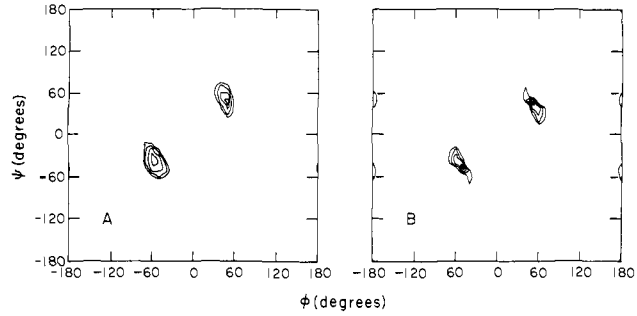

Figure 3. Conformational energy contour maps of regularly repeating conformations ($\phi_1 = \phi_2 = \phi_3$) and ($\psi_1 = \psi_2 = \psi_3$) of Ac-Aib$_3$-NHMe for (A) asymmetric and (B) symmetric geometry, with all values of ω and χ fixed at 180°. The contour lines are drawn at 1, 5, 10 and 15 kcal/mol above the 10° grid point of lowest energy for each map, located at $(\phi,\psi) = (-60°,-30°)$ in part A and $(-50°,-50°)$ in part B. See the text for discussion of equivalent enantiomeric conformations in the case of asymmetric geometry.

conformational energy space of the blocked single residue Ac-Aib-NHMe using asymmetric and symmetric geometry, respectively. The overall conformational space available for each geometry is similar, although the high-energy C_7^{eq} region is slightly less unfavorable for the asymmetric than for the symmetric geometry. In the case of asymmetric geometry, it *appears* from the map that the two lowest energy conformations do not have the same energy. It should not be construed from this, however, that an experiment could distinguish between left- and right-handed helical forms of Ac-Aib-NHMe. As pointed out in Residue Geometry, the conformation and geometry are intimately related. Thus, if the bond angles involving C^{β}_L and C^{β}_D were reversed from those used to compute the data of Figure 1A, then the relative energies of the two lowest energy minima would be reversed. The lowest energy conformations obtained with the two choices of bond angles are mirror images of each other, and both have the same energy. Of course, symmetric geometry also leads to exact equivalence of mirror-image conformations.

The conformational space available to the backbone is more restricted in the presence of a second Aib residue, as shown in Figure 2A,B for the regularly repeating conformations. The low-energy conformational space is further reduced for Ac-Aib$_3$-NHMe, for which only two very small areas are available in the region containing the right- and left-handed 3_{10}- and α-helical conformations (Figure 3A,B). The comments made above about the equivalence of the lowest energy right- and left-handed conformations apply to the di- and tripeptide as well as for the single residue.

The minimum-energy conformations of Ac-Aib$_n$-NHMe for n = 1 and 2 are listed in Tables III and IV, respectively, and

(21) Dennis, J. E.; Mei, H. H. W. Technical Report No. 75-246, Cornell University, Ithaca, NY, 1975.
(22) Momany, F. A.; Carruthers, L. M.; McGuire, R. F.; Scheraga, H. A. *J. Phys. Chem.* **1974**, *78*, 1595–1630.

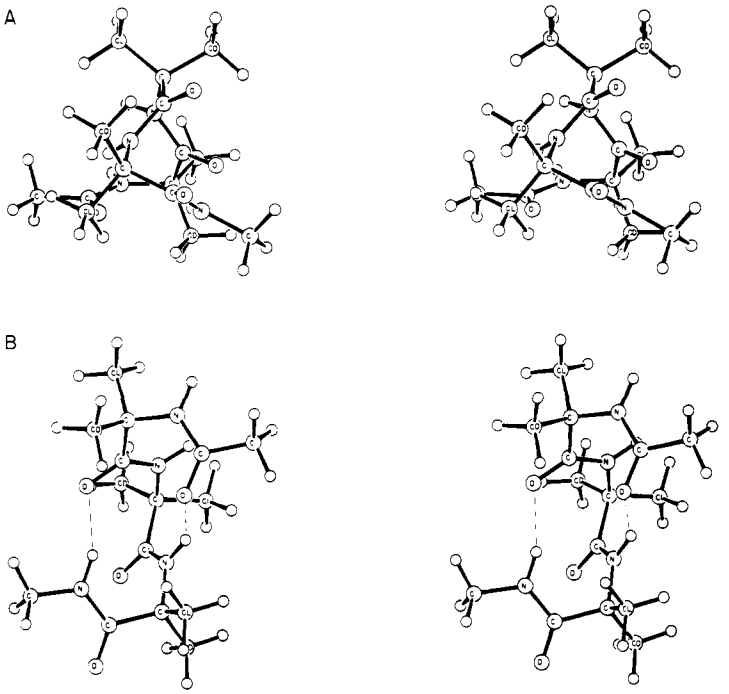

Figure 4. Stereo ORTEP diagram of the lowest energy conformation of Ac-Aib$_3$-NHMe with asymmetric geometry, a right-handed 3_{10} helix. (A) View down the helix axis. (B) View with the helix axis parallel to the page. Hydrogen bonds are shown with dashed lines. CD and CL denote the two C^β atoms (see Methods).

Table III. Minimum Energy Conformations of Ac-Aib-NHMe with $\Delta E \leq 5$ kcal/mol

dihedral angles, deg					ΔE, kcal/mol
ϕ	ψ	ω	$\chi^{1,1}$	$\chi^{1,2}$	
Asymmetric Geometry					
−55.5	−40.3	−179.7	172.6	176.5	0.000[a]
47.5	48.4	179.9	−177.7	−173.0	1.171
−62.3	171.8	−177.6	158.3	−179.0	3.153
−175.4	50.8	−179.5	−158.5	178.5	3.274
175.2	−47.1	179.3	184.3	159.6	3.754
Symmetric Geometry[b]					
−53.8	−46.4	−179.7	174.1	177.4	0.000[c]
−176.9	51.5	−179.6	−163.8	176.4	2.162
−60.9	170.5	−177.5	161.1	−179.2	3.209
−180.0	−180.0	−180.0	−175.8	175.8	4.074

[a] $E_0 = -0.127$ kcal/mol. [b] Minima for the mirror images of these conformations ($-\phi,-\psi$) are not listed. They have the same energies as those listed. [c] $E_0 = 0.635$ kcal/mol, i.e., the sum of the contributions to the energy of this conformation from electrostatic, nonbonded, and torsional terms is 0.75 kcal/mol higher than the minimum energy attainable for the asymmetric geometry (the energy of bond angle bending is not included).

marked in Figures 1 and 2. The minimum-energy conformations of Ac-Aib$_3$-NHMe are listed in Table V, but (since the values of ϕ and ψ vary between residues by up to 4°) they are not marked on Figure 3. In both the di- and the tripeptide, the dihedral angles of the lowest energy conformation with asymmetric geometry are close to those of the ideal 3_{10} helix, and the dihedral angles of the lowest energy conformation with symmetric geometry are close to those of the ideal α helix.

The two lowest energy conformations of the dipeptide with asymmetric geometry, shown in Table IV, have opposite chirality. Both have a 3_{10}-type hydrogen bond with an (N)H···O distance of 2.15 Å. The lowest energy conformation of the dipeptide with symmetric geometry, being an α-helical conformation, does not have this hydrogen bond. Hydrogen bonds exist in the minimum-energy conformations of the tripeptide in both the symmetric and the asymmetric geometries, shown in Table V. The molecule with symmetric geometry has one α-type hydrogen bond with an (N)H···O distance of 1.96 Å. There are two 3_{10}-type hydrogen bonds in each of the two lowest energy conformations with asymmetric geometry. Their (N)H···O distances are 2.19 and 2.15 Å, for the (lower energy) right-handed conformation, and 2.16 and 2.18 Å, for the left-handed conformation.

Stereo drawings from two different views of the minimum energy conformations of the *N*-acetyl-*N'*-methyl(α-aminoisobutyryl)$_3$amide, with the two geometries are shown in Figures 4 and 5, respectively. The molecule with asymmetric geometry is in the 3_{10} conformation, and the molecule with symmetric geometry is in the α-helical conformation.

The conformational energy maps for the terminally blocked single residue, using either asymmetric or symmetric geometry

Table IV. Minimum Energy Conformations of Ac-Aib$_2$-NHMe-Amide with $\Delta E \leq 5$ kcal/mol

dihedral angles, deg										ΔE, kcal/mol
first residue					second residue					
ϕ	ψ	ω	$\chi^{1,1}$	$\chi^{1,2}$	ϕ	ψ	ω	$\chi^{1,1}$	$\chi^{1,2}$	
Asymmetric Geometry										
−55.4	−36.8	−178.5	172.4	177.1	−55.1	−37.8	−178.5	172.9	176.8	0.000[a]
48.2	44.1	177.4	178.1	−171.9	48.0	45.0	178.2	−178.1	−173.7	2.512
−55.2	−39.9	179.3	172.7	176.5	47.9	47.8	−179.9	−177.8	−172.8	2.664
47.4	48.0	−178.9	−177.6	−173.0	−56.0	−39.7	−179.8	172.6	176.7	2.687
Symmetric Geometry[b]										
−54.5	−43.8	−176.5	173.5	177.7	−54.3	−44.7	−179.0	174.3	177.6	0.000[c]
53.5	45.9	181.0	−177.3	−174.2	−54.3	−45.8	−179.8	174.0	177.5	1.106

[a] $E_0 = 4.604$ kcal/mol. [b] Minima for the mirror images of these conformations ($-\phi,-\psi$) are not listed. [c] $E_0 = 6.542$ kcal/mol.

Table V. Minimum Energy Conformations of Ac-Aib$_3$-NHMe with $\Delta E \leq 5$ kcal/mol[a]

dihedral angles, deg															ΔE, kcal/mol
first residue					second residue					third residue					
ϕ	ψ	ω	$\chi^{1,1}$	$\chi^{1,2}$	ϕ	ψ	ω	$\chi^{1,1}$	$\chi^{1,2}$	ϕ	ψ	ω	$\chi^{1,1}$	$\chi^{1,2}$	
Asymmetric Geometry															
−55.3	−35.3	−176.9	172.4	177.2	−54.4	−38.4	−176.4	173.6	176.8	−57.9	−36.2	−178.6	172.3	−179.4	0.000[b]
47.8	44.0	176.2	−178.2	−172.2	48.1	45.6	174.7	−178.1	−173.0	50.6	43.3	178.4	179.1	−171.7	3.464
Symmetric Geometry[c]															
−53.9	−48.6	−177.0	−174.3	177.1	−55.5	−51.5	−176.2	174.4	176.7	−57.0	−46.0	179.4	173.2	178.3	0.000[d]

[a] There are no minima within the energy range $5 < \Delta E \leq 10$ kcal/mol. [b] $E_0 = 8.408$ kcal/mol. Stereo drawings of two views of this molecule are shown in Figure 4A,B. [c] The minimum for the mirror image of this conformation $(-\phi,-\psi)$ is not listed. [d] $E_0 = 9.655$ kcal/mol. Stereo drawings of two views of this molecule are shown in Figure 5A,B.

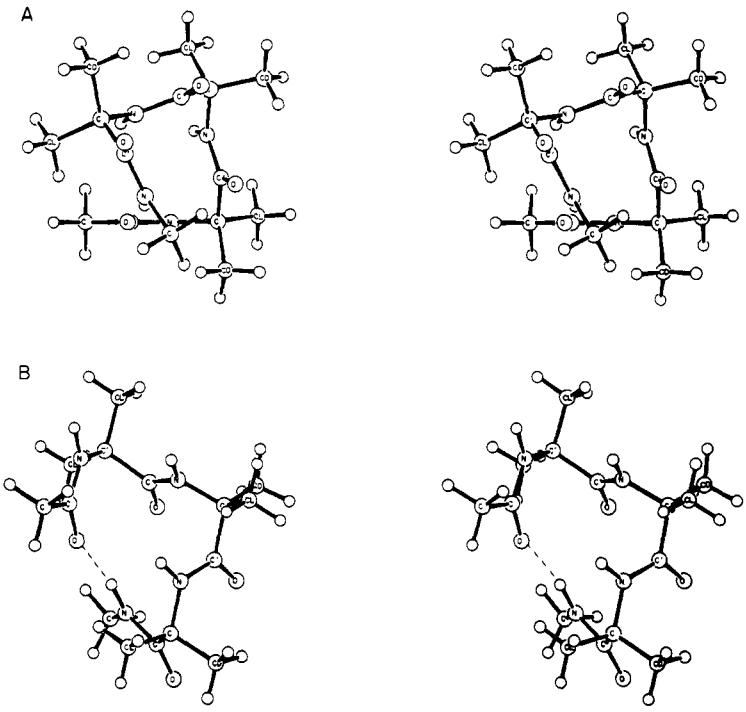

Figure 5. Stereo ORTEP diagram of the lowest energy conformation of Ac-Aib$_3$-NHMe with symmetric geometry, a right-handed α helix. (A) View down the helix axis. (B) View with the helix axis parallel to the page. The hydrogen bond is shown with a dashed line. CD and CL denote the two C^β atoms (see Methods).

and planar peptide groups (Figure 1A,B), do not differ greatly in overall appearance from each other or from those produced earlier by other workers[13-15] for Ac-Aib-NHMe. Within each low-energy area, however, energy minimization with respect to all dihedral angles leads to different minimum-energy conformations, depending on the geometry used. Energy minimization was not used in the previous studies,[13-15] and a complete description of the geometry used for the Aib residue is not given in two of them;[13,14] the third study[15] used an asymmetric geometry from an early crystal structure on the free (unblocked) amino acid. Thus, the failure of these previous studies to establish the 3_{10}-conformational preference of the Aib residue can be attributed to the sensitivity of this severely sterically restricted amino acid residue to small changes in covalent geometry.

A more recent study[16] on poly(Aib) did make allowances for changes in geometry by altering $\tau(C^\beta_L C^\alpha C^\beta_D)$ and in dihedral angles by varying ω as well as ϕ and ψ. It was demonstrated that nonplanar distortions in the peptide bond lowered the energy of both α-helical and 3_{10} conformations. These calculations showed that a distorted α helix with $i \rightarrow i-4$ hydrogen bonding was preferred over a 3_{10} helix by poly(Aib). The direction of deviation from planarity computed in the study cited[16] agrees with those obtained here. The magnitudes of the deviations[16] are larger than those that we obtained and depend strongly on the potential functions used which differ from those in this study. Therefore, only a qualitative comparison can be made with the results reported here.

Table VI. Deviations from Planarity of the Peptide Unit in the Computed Lowest Energy Conformations of Ac-Aib$_n$-NHMe, with $n = 1$, 2, and 3

		value of ω, deg		
		asymmetric geometry		symmetric geometry
n	residue no.	right-handed 3_{10} helix	left-handed 3_{10} helix	right-handed α helix[a]
1	1	−179.7	179.9	−174.7
2	1	−178.5	177.4	−176.5
	2	−178.5	178.2	−179.0
3	1	−175.9	176.2	−177.2
	2	−175.4	174.7	−175.7
	3	−178.6	178.4	−179.3

[a] Values of ω for the left-handed α helix, having the same energy, have opposite sign and the same magnitude.

We find small but significant deviations from planarity in the lowest energy conformations of the terminally blocked single residue, dipeptide, and tripeptide (Table VI). The average of the deviation from planarity, viz., of $\Delta\omega = 180° - |\omega|$, has the values $\langle\Delta\omega\rangle = 2.2 \pm 1.6°$ for the minima with asymmetric geometry and $\langle\Delta\omega\rangle = 1.8 \pm 1.8°$ for the minima with symmetric geometry. The sign of the deviation is correlated in a consistent manner (for both geometries) with the chirality of the residues,

Table VII. Deviations from Planarity of Peptide Units in X-ray Crystal Structures of Aib-Containing Peptides

peptide	ref	ω, deg	chirality of the Aib residue[a]
Ac-Aib-methylamide	7	−175.0	R
Z-Aib-Pro-NHMe	8	−174.0	R
Z-Aib-Pro-Aib-Ala-OMe	9	−175.0	R
		175.8	L
Z-Aib$_2$-Ala-OH	10	−177.7	L
Boc-Leu-Aib-Pro-OH	11	176.0	L
Boc-Pro-Aib-Ala-Aib-OBzl		−173.0	R
		−176.0	R
Z-Aib$_2$-OH	12	172.4	L
Z-Aib$_4$-OH	12	−177.6	R
		178.7	R
		179.3	R
Z-Aib$_5$-OBu^t	12	180.0	R
		−174.3	R
		−171.7	R
		−174.0	R
Tos-Aib$_5$-OMe	6	179.1	L
		173.1	L
		173.8	L
		171.7	L

[a] See footnote a of Table II.

viz., a negative value of ω is associated with a right-handed helical conformation of the residue (where φ and ψ also are negative) and a positive value of ω with a left-handed helical conformation. Apparently, the deviation serves to relieve similar constraints for residues of both chiralities. The computed results agree with observations in crystal structures of peptides containing the Aib residue in the 3_{10}-helical conformation (Table VII). In 17 out of 20 observations, the direction of deviation of ω from 180° is also correlated with the chirality of the residue, as described above. The average magnitude of the observed deviation is $\langle\Delta\omega\rangle = 4.5 \pm 3.3°$.

Effect of Covalent Geometry on Conformational Preference. The results of the conformational energy calculations on Ac-Aib$_n$-NHMe (with n = 1, 2, 3) described in the previous section establish that the choice of covalent geometry around the C^α atom for this sterically restricted molecule critically determines its conformational preference. The purpose of the work presented in this section is to establish the energetic advantages that asymmetry confers on the Aib residue in the 3_{10}-helical conformation.

The range of values of (φ,ψ) over which a hydrogen bond of a given type can be formed is obviously influenced by the value of the τ(NC$^\alpha$C′) bond angle. This bond angle increases by 1.7° from the symmetric to the asymmetric geometry. Contour plots of the 3_{10}-helical ($i \rightarrow i-3$) and α-helical ($i \rightarrow i-4$) H···O distances are shown for both geometries in Figures 6 and 7, respectively. The figures indicate that the two kinds of hydrogen bonds form in distinct regions of (φ,ψ) space. There is a region, however, in which a small change of dihedral angles, particularly of ψ, will make one hydrogen bond shorter than the other. Within the energetically allowed area ($\Delta E \leq 5$ kcal/mol) of the map for each geometry, there is about an equal distribution of α-helical and 3_{10}-helical conformations. The higher value assigned to τ(NC$^\alpha$C′) in the asymmetric geometry does not alter this distribution significantly. Thus, the preference for the 3_{10}-helical conformation, for asymmetric geometry, cannot be explained solely by the geometrical ease of formation of the hydrogen bond and must be due to the difference in the energy balance of all interactions in the two geometries, as discussed next.

A comparison of the energy components for Ac-Aib$_2$-NHMe shows that the computed energy of the 3_{10}-helical conformation is about 2.5 kcal/mol lower with the asymmetric geometry than with the symmetric geometry (Table VIII). Almost all of this energy difference resides in the nonbonded energy component. It should be noted, however, that energy differences due to straining bond angles are not included in the computations reported here. Inclusion of strain energy would raise the total energy of *all* conformations of the molecule with the fixed asymmetric geometry by a constant amount.

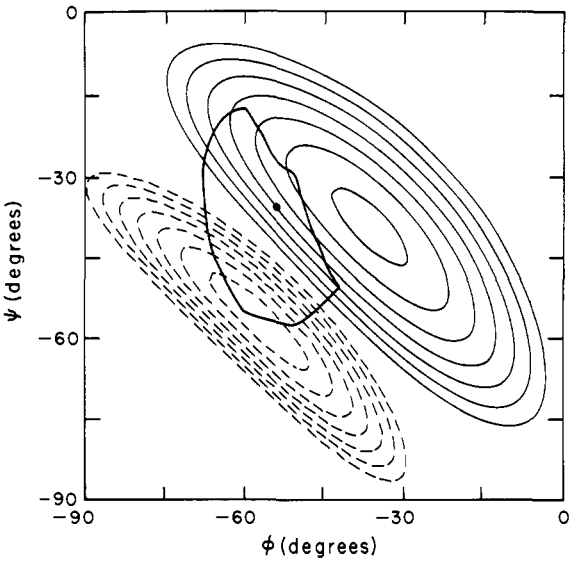

Figure 6. Contour diagram of hydrogen bond distances in the 3_{10}- and α-helical region of the (φ,ψ) map for Ac-Aib$_3$-NHMe with asymmetric geometry. Solid contours represent the (N)H$_i$···O$_{i-3}$ distance (a 3_{10}-type hydrogen bond); dashed contours represent the (N)H$_i$···O$_{i-4}$ distance (an α-helical-type hydrogen bond). The contours are drawn in 0.1-Å increments from 1.7 (the innermost contour) to 2.3 Å. The hydrogen bond distance for the tripeptide conformation of lowest energy is marked ●. The energetically allowed region of the dipeptide map ($\Delta E \leq 5$ kcal/mol) is bounded by a bold solid line.

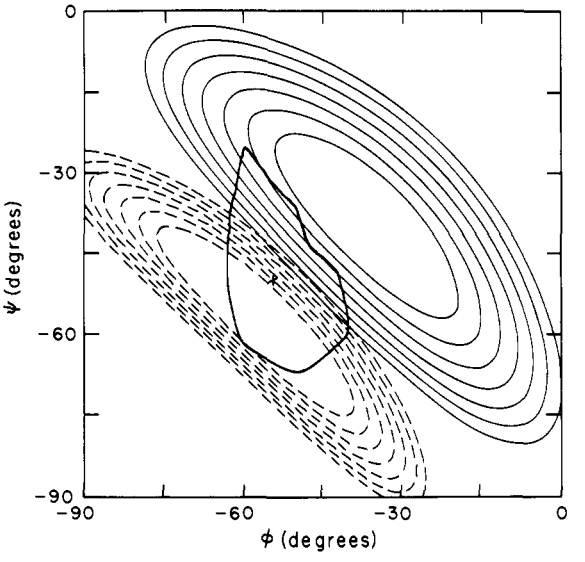

Figure 7. Contour diagram of hydrogen-bond distances in the 3_{10}- and α-helical region of the (φ,ψ) map for Ac-Aib$_3$-NHMe with symmetric geometry. Solid contours represent the (N)H$_i$···O$_{i-3}$ distance (a 3_{10}-type hydrogen bond); dashed contours represent the (N)H$_i$···O$_{i-4}$ distance (an α-helical-type hydrogen bond). The contours are drawn in 0.1-Å increments from 1.7 (the innermost contour) to 2.3 Å. The hydrogen bond distance for the tripeptide conformation of lowest energy is marked +. The energetically allowed region of this dipeptide map ($\Delta E \leq 5$ kcal/mol) is bounded by a bold solid line.

Most of the lowering in nonbonded energy for the asymmetric geometry arises from more favorable backbone-backbone interactions due to the increase in τ(NC$^\alpha$C′) (Table IX). It is presumably these favorable interactions which force the geometry to be asymmetric. On going from the symmetric to the asymmetric geometry all bond angles involving the C^β_D methyl carbon atom increase (Table II); this is the methyl substituent which is sterically

Table VIII. Energy Components for Selected Conformations of Ac-Aib$_2$-NHMe with Asymmetric and Symmetric Geometry

	dihedral angles,[a] deg				energy, kcal/mol			
	first residue		second residue					
geometry	ϕ	ψ	ϕ	ψ	E_{TOR}	E_{ES}	E_{NB}	E
asymmetric[b]	−55.4	−36.8	−55.1	−37.8	0.258	4.871	−0.525	4.604
symmetric[c]	−55.4	−36.8	−55.1	−37.8	0.260	4.997	1.819	7.076
symmetric[b]	−54.5	−43.8	−54.3	−44.7	0.237	5.522	0.784	6.542

[a] Only the dihedral angles ϕ and ψ are listed here. The values of ω, $\chi^{1,1}$, and $\chi^{1,2}$ are those in Table IV. [b] These are the computed lowest energy conformations for the two geometries. [c] This is the same conformation as the one listed in the first line; it is listed for comparative purposes and is not a minimum energy conformation for the symmetric geometry.

Table IX. Difference in Individual Nonbonded Pair Interaction Energies between Backbone Atoms in Two Adjacent Peptide Groups of Ac-Aib$_2$-NHMe for the 3_{10} Conformation[a] with Asymmetric and Symmetric Geometries

atom pair	ΔE,[b] kcal/mol
$C'_{i-1}\cdots C'_i$	−0.104
$C'_{i-1}\cdots O_i$	0.005
$C'_{i-1}\cdots N_{i+1}$	−0.201
$C'_{i-1}\cdots H(N)_{i+1}$	−0.043
$O_{i-1}\cdots C'_i$	−0.140
$O_{i-1}\cdots O_i$	−0.143
$O_{i-1}\cdots N_{i+1}$	−0.032
$O_{i-1}\cdots H(N)_{i+1}$	0.001
$N_i\cdots O_i$	0.003
$N_i\cdots N_{i+1}$	−0.304
$N_i\cdots H(N)_{i+1}$	0.035
$(N)H_i\cdots C'_i$	0.004
$(N)H_i\cdots O_i$	0.000
$(N)H_i\cdots N_{i+1}$	0.004
$(N)H_i\cdots H(N)_{i+1}$	0.002
	−0.915

[a] For the conformations listed in the first two lines of Table VIII. [b] $\Delta E = E_{NB}$(asymmetric) − E_{NB}(symmetric).

Table X. Difference in Nonbonded Interaction Energy between Hydrogen Bonded Atoms and the Backbone Atoms Bonded to them[a]

atom pair	type of interaction	ΔE,[b] kcal/mol
$O_{i-1}\cdots N_{i+2}$	nonbonded	−0.44
$O_{i-1}\cdots H(N)_{i+2}$	hydrogen bond	0.23
$C'_{i-1}\cdots H(N)_{i+2}$	nonbonded	−0.18
$C'_{i-1}\cdots N_{i+2}$	nonbonded	−0.06
		−0.45 total

[a] For the conformations listed in the first two lines of Table VIII. [b] $\Delta E = E_{NB}$(asymmetric) − E_{NB}(symmetric).

more constrained in the right-handed 3_{10}- (and α−) helical conformations. The bond angles involving the C^{β}_L methyl carbon atom, which is sterically less crowded in the conformations mentioned, decrease. These slight changes in the positions of the methyl groups with respect to the backbone atoms do not profoundly affect the *total* interaction energy of the two methyl groups with the backbone atoms (which is about 0.1 kcal/mol lower for the molecule with asymmetric geometry than with symmetric geometry). Although the interaction energy of the O_{i-1} backbone atom with the C^{β}_{Di} atom and also one of the H^{β}_{Di} atoms is lower by −0.14 and −0.22 kcal/mol, respectively, for the asymmetric geometry, this is offset by the unfavorable interactions of the C^{β}_{Li} atom with the amide H_i and N_{i+1} atoms which are higher for the asymmetric geometry by 0.26 and 0.10 kcal/mol, respectively; i.e., the side chain–backbone interactions make a minor contribution compared to the backbone–backbone interactions.

If the methyl group had been placed symmetrically with the increased $\tau(NC^{\alpha}C')$, however, all the other bond angles around the C^{α} atom would have been less than the tetrahedral value of 109.45°. The effect of this would be to increase the side chain–backbone interactions unfavorably in this sterically hindered molecule. The small changes in the side chain–backbone and side chain–side chain bond angles observed consistently in the crystal structures compiled in Table II and incorporated into the geometry of the asymmetric molecule have obviously more than compensated for these unfavorable interactions and the energy of bond angle distortion (i.e., the bond angles change in response to these interactions).

A further source of favorable energy for the asymmetric geometry occurs in the medium-range interactions between atoms O_{i-1} and $H_{i+2}(N)$, involved in a hydrogen bond, and between the backbone atoms to which they are bonded, C'_{i-1} and N_{i+2}. Table X shows the difference between the nonbonded energy for the molecule with asymmetric and symmetric geometry. Although the pairwise hydrogen bonding interaction between the donor atom H_{i+2} and the acceptor atom O_{i-1} is more favorable for the symmetric geometry because of a closer distance of approach for these two atoms (see locations of this conformation on Figures 6 and 7), the nonbonded interaction energy for the other atom pairs leads to a net decrease of the overall energy of the hydrogen bond of 0.45 kcal/mol for the asymmetric geometry.

Discussion

The X-ray crystal structural observations on Aib peptides shown in Tables I and II confirm that the use of a standard geometry [with different values of $\tau(NC^{\alpha}C')$ for each type of amino acid residue[18]] in computations[20] is a good assumption for most groups in amino acid residues. The average bond lengths shown in Table I and the peptide group bond angles in Table II are within two standard deviations of the values used in ECEPP and derived from the L-amino acids.[18] It thus appears that the use of fixed bond lengths and bond angles in empirical energy calculations on peptides is adequate in most cases. Close atomic interactions in sterically crowded structures may, however, result in deviations[23] from usual bond angles. Therefore, care must be exercised in the use of a "standard geometry" in such situations.

In the case of the Aib residue, the C^{α} atom is substituted by four heavy atoms. It might be expected that steric repulsions between these atoms would maintain a nearly symmetric[24] arrangement of the four substituents. The X-ray crystal data summarized in Table II show, however, that the geometry of the C^{α} atom of Aib is asymmetric with respect to the $C^{\beta}H_3$ groups. Since the asymmetric geometry is required to stabilize the 3_{10}-helical conformation, this conformation would be preferred in solution over the α helix only if this geometry is not peculiar to the crystal. The present study demonstrates the sensitivity of conformation to geometry and establishes the energetic advantages conferred by intramolecular nonbonded and electrostatic interactions on the Aib residue with asymmetric geometry in the 3_{10}-helical conformation. It remains to be established whether the maintenance of asymmetric geometry as observed in the crystal requires intermolecular interactions in addition to the intramolecular interactions mentioned or whether the latter are sufficient to compensate for bond angle strain in the molecule with asymmetric geometry.

(23) Benedetti, E.; Pedone, C.; Toniolo, C.; Némethy, G.; Pottle, M. S.; Scheraga, H. A. *Int. J. Pept. Protein Res.* **1980**, *16*, 156–172.

(24) Any small deviations from tetrahedral symmetry would be expected to be due to the chemical differences of the four substituents. Thus, one would expect that any asymmetry would involve the N atom or, perhaps, to a lesser extent the C′ atom, but the two $C^{\beta}H_3$ groups should behave equivalently.

Solution studies using ^1H NMR[7,9] and IR[7,25,26] spectroscopy on Aib-containing peptides of 1–6 residues have suggested that such peptides adopt well-defined structures in solution. A CD study[27] on longer peptides (7–19 residues) containing Aib and other (L-) residues reported the helical content of these peptides, but it is not possible to distinguish between 3_{10} or α helices by this method. On the basis of IR studies, C_5 and C_7 hydrogen-bonded ring structures have been suggested[7,26] as the preferred conformations of several small Aib-containing peptides that are too short to form a 3_{10}-type hydrogen bond. A type II β turn ($\phi_1 = -62°$, $\psi_1 = 137°$, $\phi_2 = 96°$, $\psi_2 = 3°$) was assigned[7] as the structure of Bu^{t}CO-Pro-Aib-NHMe; our calculations show that this conformation and the C_5 and C_7 conformations are disallowed for the single Aib residue (Figure 1) and di- and tripeptides (Figures 2 and 3). The minimum appearing in the C_7 region in the energy contour map of the single residue (Figure 1) is 6 kcal/mol higher than that for the 3_{10} conformation, even after minimization with respect to all dihedral angles. It is possible that the hydrogen bonding detected in solutions of small Aib-containing peptides[7,26] using IR is intermolecular rather than intramolecular. An increase in the number of hydrogen bonds with an increase in the length of the oligopeptide chain in a series of Aib-containing peptides[26] was attributed to incipient 3_{10} helices of increasing length. Integrated intensities of the hydrogen bonded N–H stretching band were used to obtain a quantitative estimate of the number of hydrogen bonds.[26] The assumption was made, however, that an $i \rightarrow i-3$ bond was the only hydrogen bond likely for this molecule; if the possibility of an $i \rightarrow i-4$ hydrogen bond is admitted, then the same increase in the number of hydrogen bonds for this series of oligopeptides would be expected with incipient α-helix formation, and hence the experiment cannot exclude α-helices.

Stronger evidence for formation of 3_{10}-type ($i \rightarrow i-3$) hydrogen bonds in small Aib-containing peptides is provided by a ^1H NMR study[9] on Z-Aib-Pro-Aib-OMe and Z-Aib-Pro-Aib-Ala-OMe. The former molecule is incapable of forming an α-helical hydrogen bond but can form a 3_{10}-type hydrogen bond. The rates of exchange of the various amide and urethane hydrogens in these molecules were measured by monitoring the disappearance of the corresponding proton resonances on addition of D_2O. All but the $H(N)_{i+2}$ of the tripeptide and the $H(N)_{i+2}$ and $H(N)_{i+3}$ of the tetrapeptide exchanged in minutes. These protons took several hours to exchange with deuterium, presumably because they were hydrogen bonded.

Further experimental studies are required to establish whether Aib universally adopts the 3_{10} conformation in solution—as it appears to do in crystal structures. If this is the case, the calculations presented in this study would suggest that the asymmetric geometry that the Aib residue adopts in the crystalline state also prevails in solution.

Acknowledgment. We are indebted to M. S. Pottle for expert advice in computing and Dr. G. D. Smith for making data available to us prior to publication. This work was supported by research grants from the National Science Foundation (PCM79-20279), the National Institute of General Medical Sciences (GM-14312), and the National Institute on Aging (AG-0322) of the National Institutes of Health, U.S. Public Health Service, and by a NATO research grant (No. 1616).

(25) Rao, Ch. P.; Nagaraj, R.; Rao, C. N. R.; Balaram, P. *FEBS Lett.* **1979**, *100*, 244–248.
(26) Rao, Ch. P.; Nagaraj, R.; Rao, C. N. R.; Balaram, P. *Biochemistry* **1980**, *19*, 425–431.
(27) Oekonomopulos, R.; Jung, G. *Biopolymers* **1980**, *19*, 203–214.

Theoretical Calculations on Proton-Transfer Energetics: Studies of Methanol, Imidazole, Formic Acid, and Methanethiol as Models for the Serine and Cysteine Proteases

Peter A. Kollman* and David M. Hayes

Contribution from the Department of Pharmaceutical Chemistry, School of Pharmacy, University of California, San Francisco, California 94143. *Received February 25, 1980*

Abstract: We present ab initio calculations on the proton-transfer energetics for models of the serine and cysteine protease "charge-relay systems". The models chosen for these systems include formate···imidazole···methanol and formate··· imidazole···methanethiol and the proton-transfer isomers of these complexes. Complete optimization of the monomers and optimization of the molecule–molecule distance in dimeric complexes was carried out with an STO-3G basis set, with single-point calculations on the above trimers. Because of the well-known defects of this basis set in treating ionic molecules, we carried out a number of calculations with the 4-31G basis set. In view of the size of the systems considered, we attempted to model the above complexes at the 4-31G level by using only dimer energy surfaces, with three-body effects determined from the STO-3G and 4-31G calculations on model systems. We then validated this approach with explicit 4-31G calculations on the serine protease trimers. In contrast to previous theoretical calculations, we conclude that Asp 102 in the serine-charge-relay triad is likely to stay unprotonated during catalysis.

The serine proteases enzymes, which catalyze the hydrolysis of amide and ester bonds, have been the subject of many experimental and theoretical studies. One of the most intriguing aspect of these studies is that the enzymes α-chymotrypsin and subtilisin, which have very different primary structures, both have a "charge-relay triad" serine-histidine-aspartate in the active site[1,2] (see Figure 1). It has been assumed that the mechanism of catalysis by these enzymes is identical and that this charge-relay triad is what makes the alcoholic oxygen of serine a significantly better nucleophile than it is in aqueous solution.

Papain[3] and thiosubtilisin[4] have also been subjects of many theoretical and experimental studies; these enzymes presumably involve a sulfur as a nucleophile in place of the oxygen. In the

(1) Blow, D. M.; Birkhoft, J. J.; Hartley, B. S. *Nature (London)* **1969**, *221*, 337.
(2) Kraut, J.; Robertus, J.; Birkhoft, J.; Alden, B.; Wilcox, R.; Powers, J. *Cold Spring Harbor Symp. Quant. Biol.* **1971**, *36*, 117.
(3) Drenth, J.; Jansonius, J.; Koekock, R.; Wolthers, B. *Adv. Protein Chem.* **1971**, *25*, 79.
(4) Alden, R. A.; Wright, C. S.; Westfall, F. C.; Kraut, J. "Structure and Function Relationships of Proteolytic Enzymes"; Desmuelle, P., Neurath, H., Otteson, M., Ed.; Academic Press: New York, 1970; p 173.

0002-7863/81/1503-2955$01.25/0